Review scientific paper

Informacije MIDEM
Journal of Microelectronics,
Electronic Components and Materials
Vol. 46, No. 3(2016), 113 – 119

Micromachining of All-Fiber Photonic Micro-Structures for Microfluidic Applications

Simon Pevec[1], Borut Lenardič[2] and Denis Đonlagić[1]

[1]University of Maribor, Faculty of Electrical Engineering and Computer Science, Maribor, Slovenia
[2]Optacore d.o.o., Ljubljana, Slovenia

Abstract: Maskless micromachining of all-fiber photonics' structures, based on the selective etching of structure forming optical fibers (SFF) is presented. A maskless micromachining process can reform or reshape a section of an optical fiber into a complex 3D photonic microstructure. This proposed micromachining process is based on the introduction of phosphorus pentoxide (P2O5) into silica glass through standard fiber manufacturing technology. Micro-machining is presented as a highly effective tool for the realization of new solutions in the design of optical sensors and microfluidic devices.

Keywords: Micromachining; optical fibers; optical sensors; phosphorus pentoxide; selective etching; microstructures.

Mikroobdelava povsem vlakenskih fotonskih mikrostruktur za področje mikrofluidnih aplikacij

Izvleček: Predstavljena je mikroobdelava na osnovi selektivnega jedkanja posebnega optičnega vlakna v namene izdelave mikrofotonskih struktur. Proces mikroobdelave brez maskiranja sloni na vgradnji fosforjevega pentoksida (P_2O_5) v steklena optična vlakna skozi postopek standardne proizvodnje optičnih vlaken. Mikroobdelava je predstavljena kot zelo učinkovito orodje za realizacijo novih rešitev na področju načrtovanja senzorjev in mikrofluidnih naprav.

Ključne besede: Mikroobdelava; optična vlakna; optični senzorji; fosforjev pentoksid; selektivno jedkanje; mikrostrukture.

** Corresponding Author's e-mail: simon.pevec@um.si*

1 Introduction

Photonic micro-structures are being increasingly used in a number of applications, ranging from optical telecommunications [1-3] to biomedical sensor [4-6]. Direct implementation of micro-devices can extend their use and allow many important advantages and novel functionality. Existing solutions for optical fiber micromachining are mostly based on laser techniques. Reshaping of SiO_2 optical fiber is typically realized by laser sources operating in ultraviolet (UV) or middle-infrared (MIR), where they have sufficient absorption of light in the SiO_2 [7]. UV excimer lasers [8, 9] and femtosecond lasers [10-14] have been successfully applied as efficient tool for optical fiber micromachining. However all direct laser techniques have a common need for individual and precision guiding of the laser beam over cylindrical optical fiber, which is complex, expensive and time-consuming task. Beside laser techniques, there are also other techniques like lithographic processes [15, 16], micromachining by dry etching [17] and by focused ion beam [18-21]. Lithographic process requires many process steps, dry etching is related with time-consuming and low selectivity etching, focused ion beam technique is also time-consuming and cost-inefficient and as such unsuitable for production.

This paper presents a cost effective, mask-less micromachining process that can re-shape a section of an optical fiber into a complex 3D photonic microstructure. Micromachining based on selective etching provides a unique way for efficient design and production of complex 3D photonic all-fiber microstructures and devices [22-25]. The selective chemical etching utilizes a phenomenon where the introduction of dopants into

silica glass affects the etching rate of the glass when exposed to etching solution (usually HF). When purposely designed and properly doped optical fibers are combined/fusion spliced with standard fibers, selective etching can be exploited for the manufacturing of micro-structures on the tip, along or within the optical fibers. Structures produced by this process are made entirely of silica glass, do not utilize any adhesives or foreign materials, and can thus sustain harsh chemical and temperature conditions. Thus selective etching based micromachining involves production of SFF that involves preform production, mechanical reshaping of the preform and fiber drawing, fusion-splicing of these fibers with standard fibers, and etching of such assemblies into final photonics microstructures or devices. Thus after proper SFF production, the device production is accomplished by a sequence of fiber cleave and splice sequence(s) that are followed by (wet) etching.

This proposed micromachining process is mainly based on the introduction of P_2O_5 into silica, which can be effectively removed upon exposing the fiber to the etching medium. These preferentially etchable P_2O_5 doped areas within the fiber cross section can thus serve as sacrificial layers, thus allowing for the economical creation of complex all-fiber devices, which will be presented as result of proposed micromachining technology.

2 Etching solutions and etching selectivity

Etching selectivity S of doped region is defined as the ratio between the etching rate of the doped (v_{xx}), and that of the pure silica (v_{SiO2}).

$$S = \frac{v_{xx}}{v_{SiO_2}} \tag{1}$$

The *S* depends on the dopant type, dopant concentration, etching medium and temperature. During investigation several differently doped fiber preforms contained between one and five different doped layers of P_2O_5 concentrations were produced to study the impact of P_2O_5.

Preforms with known refractive index profiles (one typical refractive index profile is shown in Fig. 1) were in first step cut into approximately 1 to 2 cm long samples using a low speed diamond saw. The samples were then etched in etching medium. Depending on the composition of the doped glass, an etching time of between 1 min and 3 h was used to obtain well-defined surface relief. The etching vessel was temperature stabilized and

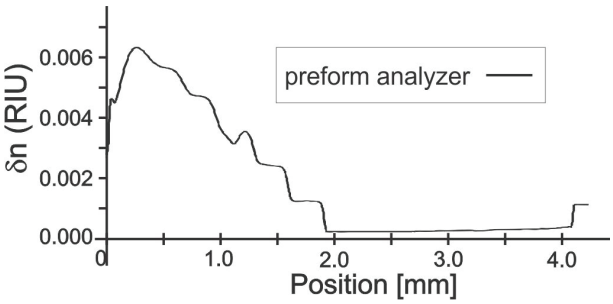

Figure 1: Preform analyzer data obtained after MCVD preform production.

also vibrated to provide acid-mixing and the removal of etching by-products from the sample's surface. The etched-preform samples were then cut in the axial direction through their centers, and were then analyzed/measured under an optical microscope. An example of such an etched preform measurement is shown in Fig. 2. The initial preform diameter and dimensions of the removed doped region were then used to determine the average v_{xx}/v_{SiO2} ratio of the individual layers of etched preform.

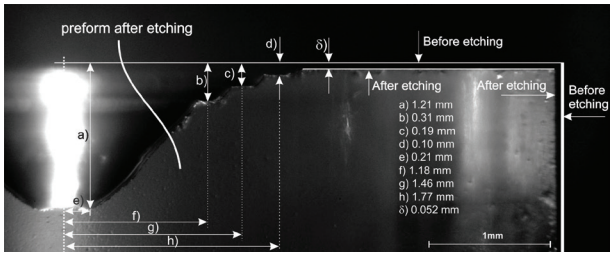

Figure 2: Selectivity measurement of P_2O_5 doped preform obtained by comparison of geometrical shape of preform before and after etching.

The preform analyzer data and the etching data were then combined to obtain a relationship between the etching selectivity S and the refractive index change caused by doping, which was further correlated to the dopant molar concentration [26].

Some dopants strongly increase *S*, while the others provide limited effect on the *S* at comparable concentration levels. From all researched dopants, P_2O_5 proved to be of particular interest for fiber micromachining. As shown in Fig. 3, the P_2O_5 doping of silica can provide very high etching selectivity S, even at low P_2O_5 concentrations. Composition of an etching agent can also strongly influence the etching selectivity. Other dopants can provide other benefits, such as strong index increase whilst providing very limited impact on the S (e.g. TiO_2).

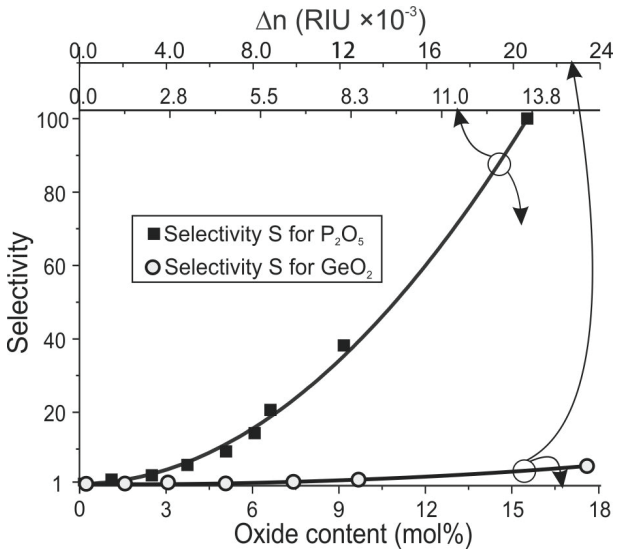

Figure 3: Selectivity as a function of P_2O_5 and GeO_2 in 40 % hydrofluoric acid at 25°C.

Great impact on selectivity has also temperature of hydrofluoric acid (HF), where by reducing the temperature from 40 to -25 °C, selectivity of P_2O_5 doped sample with higher dopant concentration (7.9 mol %) is increased from 28 to 39 as shown in Fig. 4.

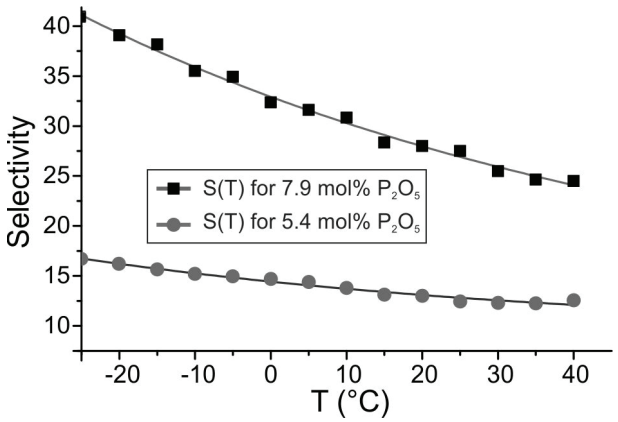

Figure 4: Selectivity as a function of temperature for two different P_2O_5 doped preform, etched in 40 % HF.

Reducing the temperature has also negative impact on etching process, because it significantly slows down the absolute etching rate and thus increase the time required for the formation of the microstructure. Furthermore by adding isopropyl-alcohol (IPA) to HF, IPA-HF etching solutions work particularly well in combination with P_2O_5 doping where doubling or even tripling of the etching selectivity can be achieved.

3 Micromachining of all-fiber photonics devices

Fiber devices are created by splicing short section of SFF at the end-of lead or in-between two lead fibers. One, very simple example produced by selective etching based on P_2O_5 doping is shown in Fig. 6. Here the micro-resonator on the optical fiber tip is presented. Micro-resonators have found applications within various photonic systems [27] such as sensors, filters, coupling devices, etc., but are difficult to produce. A cross section of the SFF, used for creation of resonator, is shown in Fig. 5 and consists of pure silica core, a large P_2O_5 region (5.7 mol%), and a thin pure SiO_2 outer-layer with the same glass transition temperature as the lead-in fiber-cladding and, thus, allows for straightforward splicing between them.

In this case the SFF was spliced between two coreless fibers, where the second coreless fiber was shortened to a length of about 15 μm as shown in Fig. 6b and then etched for sufficient time in HF.

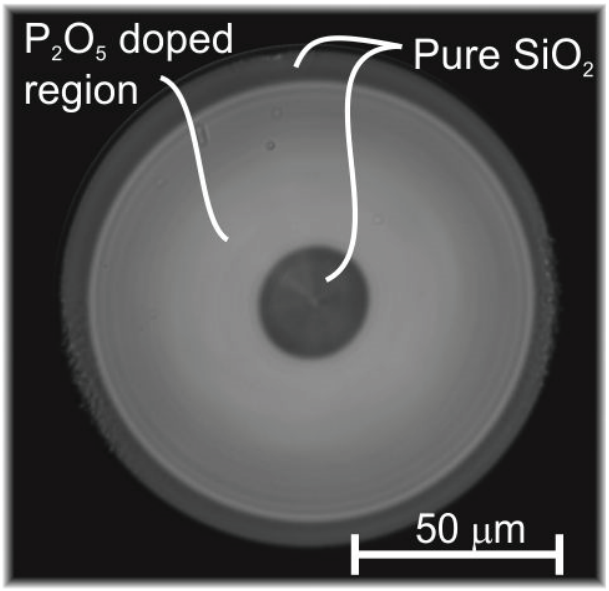

Figure 5: Optical microscopic cross-sectional view of SFF intended for micro-structure formation.

The etchant first uniformly etched the entire structure, but once the pure silica outer-layer of the SFF was removed and HF came into contact with the P_2O_5-doped region, it preferentially removed this region entirely, leaving behind the final structure shown in Fig. 6a. The total etching time was 12 min in 40 % HF at 25 °C.

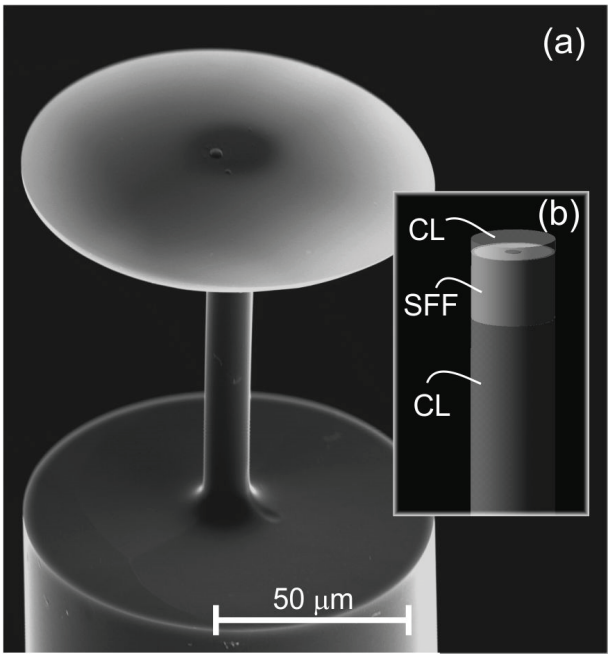

Figure 6: (a) Scanning electron microscope view of the produced micro-resonator, (b) Fiber structure before etching (after cleaving and splicing).

Depending of the device design, etching of SFF can be performed before or after splicing. Below are given few more typical examples of structures produced by application of splicing, cleaving and etching of SFFs.

The first device shown in Fig. 7a is an all-fiber optical microcell that allows for the direct insertion of liquids, gases or solids within the optical path of the transmission fiber. The micro-cell can be used as a transmission cell or as a miniature Fabry-Perot resonator. The total transmission loss of the microcell in Fig. 7a was less than 1 dB at 1550 nm, when immersed in water. Various lengths of micro-cells can be produced ranging from few tenths to few 1000 μm.

Another example device that can be effectively produced by this method is shown in Fig. 7b, and presents a miniature, all-silica, dual-parameter Fabry-Perot sensor for simultaneous measurement of surrounding fluid's refractive index (RI) and temperature. This sensor permits a full temperature-compensated high resolution RI measurement in range of 10^{-7} RIU, that can be used to determine very small changes in fluid structure or composition. All-silica design provides high chemical and thermal inertness, while the miniature size provides opportunities for measuring very small (nL) fluid volumes.

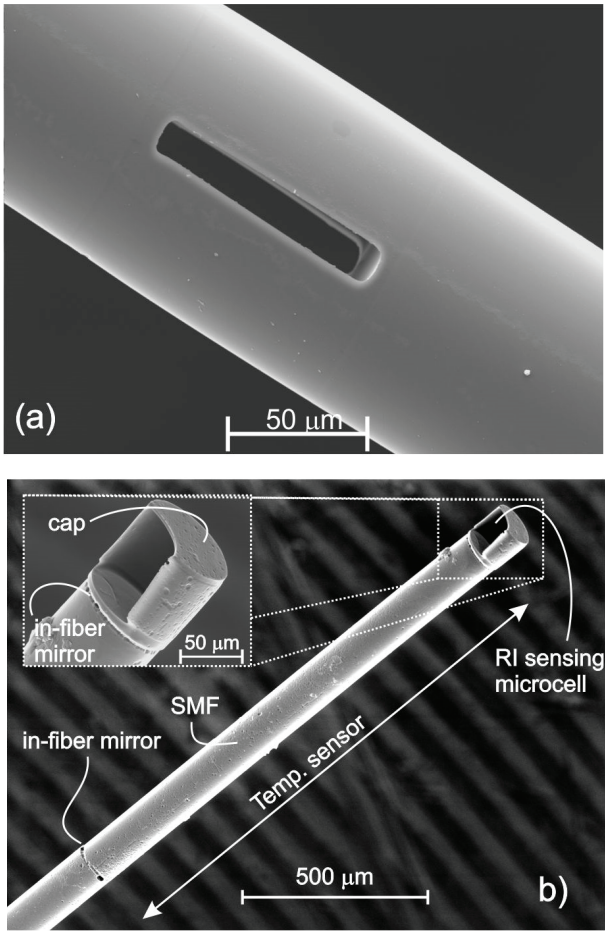

Figure 7: Microstructure devices: (a) Microcell [28], (b) Refractive index – temperature sensor [29].

Next example shown in Fig. 8a presents an all glass, Fabry-Perot, fiber–optic pressure sensor. It is the world's smallest commercial available pressure sensor [30], with outer diameter less than 125 μm, and is produced by proposed technology in few sequential steps on the tip of multi-mode lead-in optical fiber. Membrane thickness for typical pressure sensor is round 2 μm, which allow high pressure sensitivity needed for medical performance requirements. A sensitivity of 1100 nm/bar was also achieved which is, to our knowledge, the highest all-glass miniature sensor sensitivity reported in the literature. This robust sensor also demonstrated very high resistance to overload, which is an important advantage for practical usage of the sensor in realistic applications. The proposed miniature all-glass pressure sensor design is, therefore, a good candidate for applications where size, cost, material inertness, mechanical and chemical resistance as well as insensitivity to electromagnetic interferences are important concerns. Beside all advantages coming from all silica glass optical fiber design, this sensor can achieve high resolution and repeatability, very low drift, and fast response time.

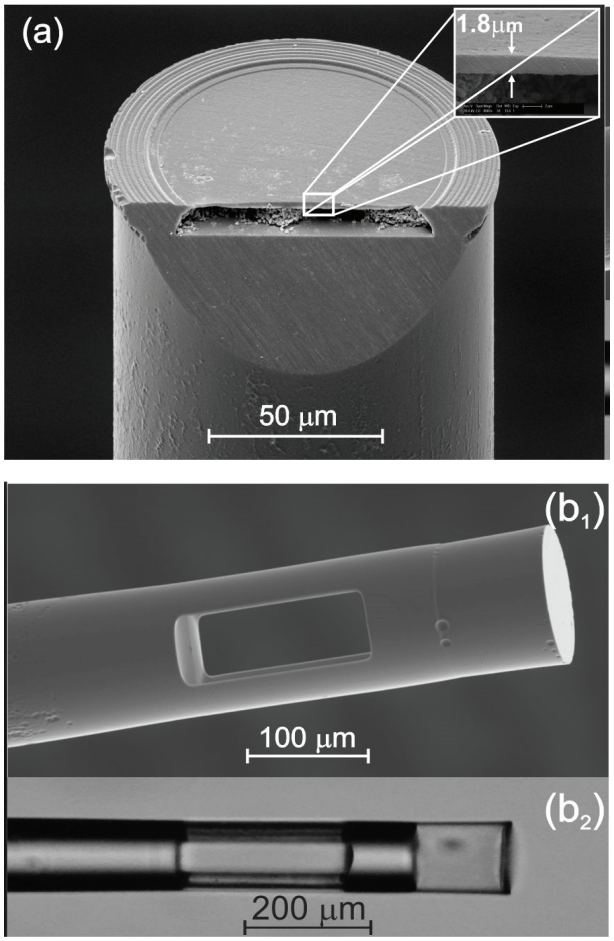

Figure 8: Microstructure devices: (a) Pressure sensor [31], (b_1) SEM photo and (b_2) optical microscope photo of Pressure – refractive index sensor respectively [32].

Another example shows one of more complex devices that can be produced by proposed technology, where microcell with pressure sensor was joined in series; it is multi parameter (multi cavity) Fabry-Perot sensor for simultaneous measurements of pressure and refractive index. Figure 8 (b_1) shows scanning microscope (SEM) image, and Fig. 8 (b_2) shows the same sensor under an optical microscope. These sensor was created at the tip of an optical fiber with a diameter that is equal to the standard fiber diameter, and length that does not exceeded 600 μm. High measurement resolutions better than 0.1 mBar and 2x10^-5 RIU can be achieved by using spectral interrogation and a FT-based measurement algorithm.

Next example in Fig. 9a shows nanowire-based refractive index sensor created on the tip of a single mode optical fiber configured as Fabry-Perot interferometer. Proposed micromachining technique including tapering allows creation of fiber coupled silica nanowires with radius between 200 and 600 nm. Nanowire sensor is made entirely of silica and includes a mechanical structure that provides stable operation and easy handling and packaging. High measuring spectral sensitivity as 800 nm/RIU and low temperature sensitivity in water are typical sensor characteristics. Sensor might be an especially attractive platform for use in compact biochemical sensors, which utilize active surfaces, for example in various label-free detection-sensing schemes.

One more example presented in Fig. 9b shows Fabry-Perot strain sensor created on the tip of a standard multi-mode fiber. Sensor's great advantage is simplicity of its production process that includes production of SFF (inset on Fig. 9b), which is cleaved, etched, and spliced between lead fibers in order to form final sensor. Tested sensors were successfully applied to strain-measurements exceeding 3000 με, which accommodate most of requirements encountered in practical industrial applications. A strain-resolution of 0.5 με, high temperature range exceeding 650 °C, and low temperature intrinsic sensitivity below 0.04 nm/°C are typical characteristics for that kind of sensor.

The last device shown in row is miniature all-silica fiber-optic sensor for simultaneous measurements of relative humidity (RH) and temperature. The sensor is composed of two cascaded Fabry-Perot interferometers (FPIs) as shown in Fig. 9c. The first FPI consists of a short silica micro-wire (diameter is cca. 13 μm) coated by a thin layer of porous silica, and forms a RH sensing part. The second section created on the sensor tip forms a temperature measuring part. The typical total length of produced sensor is less than 2 mm, while diameter doesn't exceed 125 μm. The sensor has good dynamic performances (rise time in few second range), it cover broad RH measuring range (0-100 %RH), and has linear characteristics for both measurement parameters with sensitivity of 0.48 degree/%RH and 3.7 degree/°C.

All sensors and devices have all glass structure, high environmental robustness, and a miniature design, which in any of the cases does not exceed the diameter of a standard optical fiber (i.e. 125 μm) and has an active length of less than 1.5 mm (more details can be found in appropriate references). All devices are robust and allow easy handling and packaging, especially those designed and fabricated on the tip of the optical fiber. Small dimensions, chemical resistance and robustness make sensors suitable for microfluidic applications.

Since a single customized SFF production may result in the manufacturing of a large number of devices, the proposed process potentially presents a versatile and cost-efficient way of producing all-fiber devices or device sub-assemblies.

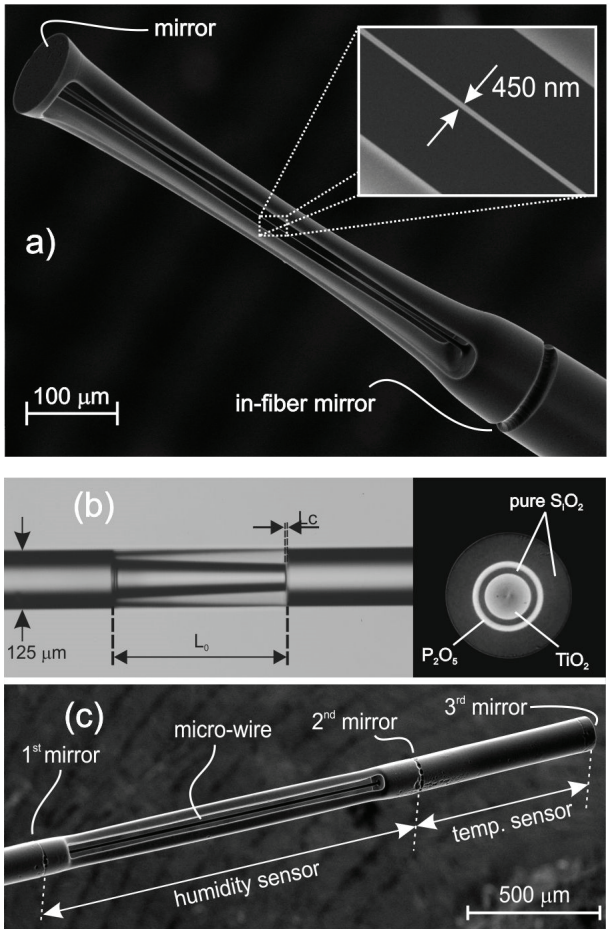

Figure 9: Microstructure devices: (a) Nano-wire refractive index sensor [33], (b) Strain sensor [34], and (c) Relative humidity – temperature sensor [35].

4 Conclusions

An effective technique for production of all fiber devices through application of selective etching and specially designed SFF was presented. The proposed technique provides versatile and potential cost-efficient way of all fiber device manufacturing through design and production of specialty SFFs.

5 Acknowledgments

Authors would like to thank to Slovenian research agency (Grant No. P2-0368 and L2-5494) and Optacore team for supplying specialty fiber required for the sensor production.

6 References

1. H. Toshiyoshi, "Micro electro mechanical devices for fiber optic telecommunication," Jsme Int J B-Fluid T 47, 439-446 (2004).
2. A. Q. Liu and X. M. Zhang, "A review of MEMS external-cavity tunable lasers," J Micromech Microeng 17, R1-R13 (2007).
3. W. H. Ko, "Trends and frontiers of MEMS," Sensor Actuat a-Phys 136, 62-67 (2007).
4. X. D. Hoa, A. G. Kirk, and M. Tabrizian, "Towards integrated and sensitive surface plasmon resonance biosensors: A review of recent progress," Biosens Bioelectron 23, 151-160 (2007).
5. T. Takahata, K. Matsumoto, and I. Shimoyama, "A wide wavelength range optical switch using a flexible photonic crystal waveguide and silicon rods," J Micromech Microeng 20(2010).
6. R. Bashir, "BioMEMS: state-of-the-art in detection, opportunities and prospects," Adv Drug Deliver Rev 56, 1565-1586 (2004).
7. R. Kitamura, L. Pilon, and M. Jonasz, "Optical constants of silica glass from extreme ultraviolet to far infrared at near room temperature," Appl Optics 46, 8118-8133 (2007).
8. J. Greuters and N. H. Rizvi, "Laser micromachining of optical materials with a 157nm fluorine laser," P Soc Photo-Opt Ins 4941, 77-83 (2003).
9. Z. L. Ran, Y. J. Rao, H. Y. Deng, and X. Liao, "Miniature in-line photonic crystal fiber etalon fabricated by 157 nm laser micromachining," Opt Lett 32, 3071-3073 (2007).
10. G. Della Valle, R. Osellame, and P. Laporta, "Micromachining of photonic devices by femtosecond laser pulses," J Opt a-Pure Appl Op 11(2009).
11. I. B. Sohn, M. S. Lee, J. S. Woo, S. M. Lee, and J. Y. Chung, "Fabrication of photonic devices directly written within glass using a femtosecond laser," Opt Express 13, 4224-4229 (2005).
12. Y. J. Rao, M. Deng, D. W. Duan, X. C. Yang, T. Zhu, and G. H. Cheng, "Micro Fabry-Perot interferometers in silica fibers machined by femtosecond laser," Opt Express 15, 14123-14128 (2007).
13. T. Wei, Y. K. Han, H. L. Tsai, and H. Xiao, "Miniaturized fiber inline Fabry-Perot interferometer fabricated with a femtosecond laser," Opt Lett 33, 536-538 (2008).
14. A. A. Said, M. Dugan, S. de Man, and D. Iannuzzi, "Carving fiber-top cantilevers with femtosecond laser micromachining," J Micromech Microeng 18(2008).
15. C. Liberale, G. Cojoc, P. Candeloro, G. Das, F. Gentile, F. De Angelis, and E. Di Fabrizio, "Micro-Optics Fabrication on Top of Optical Fibers Using Two-Photon Lithography," Ieee Photonic Tech L 22, 474-476 (2010).

16. H. Guckel, "High-aspect-ratio micromachining via deep x-ray lithography," P Ieee 86, 1586-1593 (1998).
17. J. Bierlich, J. Kobelke, D. Brand, K. Kirch, J. Dellith, and H. Bartelt, "Nanoscopic Tip Sensors Fabricated by Gas Phase Etching of Optical Glass Fibers," Photonic Sensor 2, 331-339 (2012).
18. Y. K. Kim, A. J. Danner, J. J. Raftery, and K. D. Choquette, "Focused ion beam nanopatterning for optoelectronic device fabrication," Ieee J Sel Top Quant 11, 1292-1298 (2005).
19. P. Olivero, S. Rubanov, P. Reichart, B. C. Gibson, S. T. Huntington, J. Rabeau, A. D. Greentree, J. Salzman, D. Moore, D. N. Jamieson, and S. Prawer, "Ion-beam-assisted lift-off technique for three-dimensional micromachining of freestanding single-crystal diamond," Adv Mater 17, 2427-+ (2005).
20. D. Iannuzzi, S. de Man, C. J. Alberts, J. W. Berenschot, M. C. Elwenspoek, A. A. Said, and M. Dugan, "Fiber-top micromachined devices - art. no. 700403," 19th International Conference on Optical Fibre Sensors, Pts 1 and 2 7004, 403-403 (2008).
21. D. Iannuzzi, S. Deladi, V. J. Gadgil, R. G. P. Sanders, H. Schreuders, and M. C. Elwenspoek, "Monolithic fiber-top sensor for critical environments and standard applications," Appl Phys Lett 88(2006).
22. M. S. Ferreira, J. Bierlich, S. Unger, K. Schuster, J. L. Santos, and O. Frazao, "Post-Processing of Fabry-Perot Microcavity Tip Sensor," Ieee Photonic Tech L 25, 1593-1596 (2013).
23. S. Mononobe and M. Ohtsu, "Fabrication of a pencil-shaped fiber probe for near-field optics by selective chemical etching (vol 14, pg 2231, 1996)," J Lightwave Technol 15, 162-162 (1997).
24. S. Pevec, E. Cibula, B. Lenardic, and D. Donlagic, "Micromachining of Optical Fibers Using Selective Etching Based on Phosphorus Pentoxide Doping," Ieee Photonics J 3, 627-632 (2011).
25. R. M. Andre, S. Pevec, M. Becker, J. Dellith, M. Rothhardt, M. B. Marques, D. Donlagic, H. Bartelt, and O. Frazao, "Focused ion beam post-processing of optical fiber Fabry-Perot cavities for sensing applications," Opt Express 22, 13102-13108 (2014).
26. M. M. Bubnov, M. E. Dianov, O. N. Ogorova, S. L. Semjonov, A. N. Guryanov, V. F. Khopin, and E. M. DeLiso, "Fabrication and investigation of single-mode highly phosphorus-doped fibers for Raman lasers," in *Proc. SPIE,* (2000), pp. 12-22.
27. T. M. Benson, S. V. Boriskina, P. Sewell, A. Vukovic, S. C. Greedy, and A. I. Nosich, "Micro-optical resonators for microlasers and integrated optoelectronics - Recent advances and future challenges," Nato Sci Ser Ii-Math 216, 39-70 (2006).
28. D. Donlagic, "All-fiber micromachined microcell," Opt Lett 36, 3148-3150 (2011).
29. S. Pevec and D. Donlagic, "High resolution, all-fiber, micro-machined sensor for simultaneous measurement of refractive index and temperature," Opt Express 22, 16241-16253 (2014).
30. "World-class fiber optic sensing solutions", retrieved www.fiso.com.
31. E. Cibula, S. Pevec, B. Lenardic, E. Pinet, and D. Donlagic, "Miniature all-glass robust pressure sensor," Opt Express 17, 5098-5106 (2009).
32. S. Pevec and D. Donlagic, "Miniature fiber-optic sensor for simultaneous measurement of pressure and refractive index," Opt Lett 39, 6221-6224 (2014).
33. S. Pevec and D. Donlagic, "Nanowire-based refractive index sensor on the tip of an optical fiber," Appl Phys Lett 102(2013).
34. S. Pevec and D. Donlagic, "All-fiber, long-active-length Fabry-Perot strain sensor," Opt Express 19, 15641-15651 (2011).
35. S. Pevec and D. Donlagic, "Miniature all-silica fiber-optic sensor for simultaneous measurement of relative humidity and temperature," Opt Lett 40, 5646-5649 (2015).

Arrived: 31. 08. 2016
Accepted: 22. 09. 2016